Ferromagnetism in Mn-Doped GaN Nanowires

Q. Wang, Q. Sun, and P. Jena

Physics Department, Virginia Commonwealth University, Richmond, Virginia 23284, USA

(Received 7 June 2005; published 10 October 2005)

Using density functional theory we show that the magnetic coupling of Mn atoms in the nanowires, unlike that in the thin film, is ferromagnetic. This ferromagnetic coupling, brought about due to the confinement of electrons in the radial direction and the curvature of the Mn-doped GaN nanowires' surface, is mediated by N as is evidenced from the overlap between Mn $3d$ and N $2p$ states. Calculations of the anisotropic energy further show that the magnetic moment orients preferably along the $[10\bar{1}0]$ direction while the wire axis points along the [0001] direction.

DOI: 10.1103/PhysRevLett.95.167202 PACS numbers: 75.50.Pp, 36.40.Cg, 61.46.+w, 75.75.+a

Recently there has been considerable interest in the study of dilute magnetic semiconductors (DMS) as these represent a unique class of systems where both the charge and spin of the electron can be manipulated simultaneously. Numerous investigations carried out on Mn-doped GaN [1–19] have led to conflicting results. While some experiments find the materials to be ferromagnetic (FM) [1–12], others suggest antiferromagnetic (AFM) or spin glass behavior. Among those who find Mn-doped GaN to be ferromagnetic, there is no unanimous agreement concerning the Curie temperature as the reported values range from 10 K to about 945 K. It is widely believed that sample conditions are important, and structural defects as well as secondary phases which commonly exist in thin films may be responsible for these different results.

With the advancement of experimental techniques, it has recently been possible to synthesize low-dimensional GaN-based nanostructures including nanowires and nanorods. Potential applications of these one dimensional semiconductors in lasers, transistors, and spintronics devices [20,21] also have fueled much of the current interest in this field. Since the first synthesis of the GaN nanowire using a carbon-nanotube-confined reaction [22], many efforts have been devoted to developing different methods for synthesizing GaN nanowires [23–28]. Most recently, three groups have succeeded in synthesizing single-crystalline Mn-doped GaN nanowires free of defects with diameters ranging from 10–100 nm and of lengths up to tens of micrometers [29–31]. More importantly, Mn-doped GaN nanowires have been found to be ferromagnetic up to 300 K and exhibit negative magnetoresistance. Thus, they represent an important class of nanometer-scale building blocks for miniaturized electronic devices with interesting electronic, optoelectronic, and magnetoelectronic properties.

A fundamental understanding of the low-dimensional FM semiconductor nanostructures is crucial for the development of spintronics devices. For example, it is important to know the sites Mn atoms occupy, how these sites are distributed, how the magnetic coupling between the Mn atoms depend on this distribution, and how these differ from Mn-doped GaN thin film. In this Letter we provide the first theoretical study of the magnetic properties of Mn-doped GaN nanowires having diameters of 1.00 nm and 0.45 nm. Note that these diameters are smaller than those synthesized experimentally (namely 10–100 nm). Since first principles calculations of wires with 10–100 nm diameters are computationally impossible, the present results can demonstrate the role of surface curvature and the radial confinement of the electrons on magnetism.

The GaN nanowire of 1.0 nm diameter has been generated from a bulk GaN ($7 \times 7 \times 2$) supercell having the wurtzite structure by cutting the outside part of the circled area in Fig. 1(a) along the [0001] direction. The supercell consists of 96 atoms ($Ga_{48}N_{48}$) and has about 12 Å vacuum space along the $[10\bar{1}0]$ and $[01\bar{1}0]$ directions to prevent the nanowire to interact with its image. The nanowire has infinite length along the [0001] direction, as shown in Fig. 1(b). To study the magnetic coupling between Mn atoms we have replaced two of the Ga atoms with Mn. This corresponds to a 4.2% Mn doping concentration. Since it is *a priori* not clear what are the preferred sites where Mn atoms would occupy, we have tried six different configurations by varying the sites of Mn atoms on the

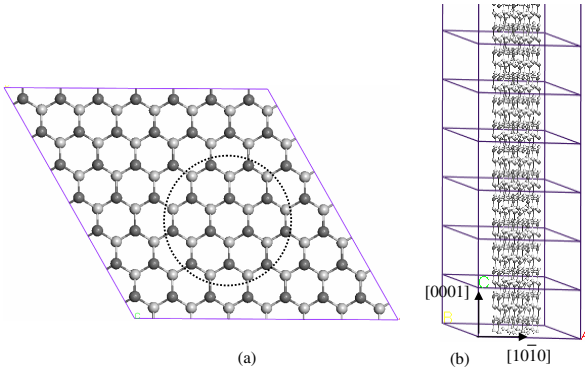

FIG. 1 (color online). (a) Top view of a $7 \times 7 \times 2$ GaN supercell having wurtzite structure. (b) $Ga_{48}N_{48}$ supercell which yields a nanowire of infinite length along [0001] direction.

outer and inner surface layers of the wire. These configurations simulate different Mn-Mn and Mn-N distances as well as Mn-N-Mn bond angles. These are shown in Fig. 2. For each of these configurations we computed the total energies corresponding to both FM and AFM alignments of the Mn spins. From the total energy minima we not only determine the preferred sites Mn atoms would occupy but also their preferred magnetic coupling. The atomic coordinates of all the atoms in the supercell were optimized without any symmetry constraint. We began with a study of the relaxation of the atoms in the nanowire without Mn incorporation. The effect of Mn doping on the magnetic properties was then calculated by first keeping the nanowire in the unperturbed bulk geometry and then by allowing all the atoms including Mn to relax. This allows us to comment on the effect of atomic relaxation on the magnetic coupling. The calculations were carried out using the Vienna *Ab initio* Simulation Package (VASP) and density functional theory [32]. The exchange and correlation potentials were calculated by using the generalized gradient approximation (GGA). We have used PW91 form [33] for the GGA. We used a plane-wave basis set and the projector augmented wave (PAW) potentials [34] for Ga, Mn, and N. The energy cutoff was set to 300 eV. The convergence in energy and force was set as 10^{-4} eV and 10^{-3} eV/Å, respectively.

We first discuss the atomic relaxation in the pure nanowire calculated by full geometry optimization of the $Ga_{48}N_{48}$ supercell. The total energy of the relaxed cell was found to be 10.628 eV lower than the unrelaxed one, corresponding to an energy gain of 0.221 eV/Ga-N dimer. The relaxed Ga-N bond length on the outermost surface layer along [0001] direction is 1.869 Å, which contracted by -5.89% compared with the bulk GaN while those in the inner two layers are 1.974 Å and 1.981 Å leading to a contraction of -0.6% and -0.05% respectively. The Ga-N bond which forms a zigzag chain on the outermost surface (approximately along $[01\bar{1}0]$ direction) changes from 1.930 Å to 1.891 Å, corresponding to a contraction of -2.02%. The corresponding angles change from $\angle$N-Ga-N = $\angle$Ga-N-Ga = 108.40° to $\angle$N-Ga-N = 118.34° and $\angle$Ga-N-Ga = 105.93°. The relaxations of the atoms in the inner sites are much smaller than those on the outermost surface layer. The nature of bond length contraction in the nanowire is similar to GaN $(11\bar{2}0)$ surface where Ga-N bond lengths contracted by -1.76% and -5.35% on the surface layer along $[10\bar{1}0]$ and [0001] directions, respectively [35].

The total electronic density of states (DOS) for spin-up and spin-down electrons corresponding to the pure GaN nanowire is plotted in Fig. 3(a). The Fermi level lies in the gap region. The DOS curves for spin-up and spin-down are completely symmetric, suggesting that the pure wire is nonmagnetic. In Table I we present the main results of our work concerning the Mn doping for all the six configurations. In the fourth column we list the relative energies $\Delta\varepsilon$ corresponding to all the six configurations of Mn measured with respect to the ground state configuration. The distances between the Mn atoms and those between Mn and nearest N atom as well as the magnetic moments at the Mn and mediating N sites are presented in the last five columns of Table I. For each configuration we also list the energy difference ΔE between the AFM and FM states (see column III). To study the effect of atomic relaxation on the magnetic coupling, we also list the results obtained by *not* allowing the system to relax (column II). Note that with the exception of configuration III, the energy difference between the FM and AFM states have the same sign whether or not the atomic relaxations were included. The negative energy means that the AFM state is lower in energy. It is apparent that the Mn atoms have a clear preference for the outermost surface sites over the interior sites since the relative energy $\Delta\varepsilon$ markedly increases when Mn atoms occupy the inner sites of the supercell.

We see that the FM state of configuration V has the lowest energy with its AFM state lying 0.075 eV above the

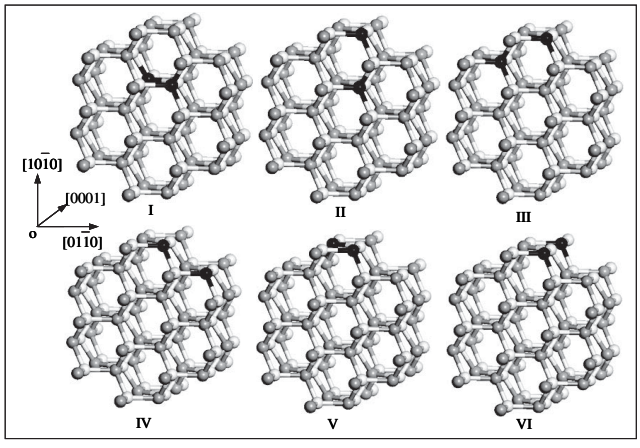

FIG. 2. Six configurations of $Ga_{46}Mn_2N_{48}$ supercell identifying various Ga sites that have been replaced by Mn. The lighter spheres are N, the gray spheres are Ga, and the black spheres are Mn.

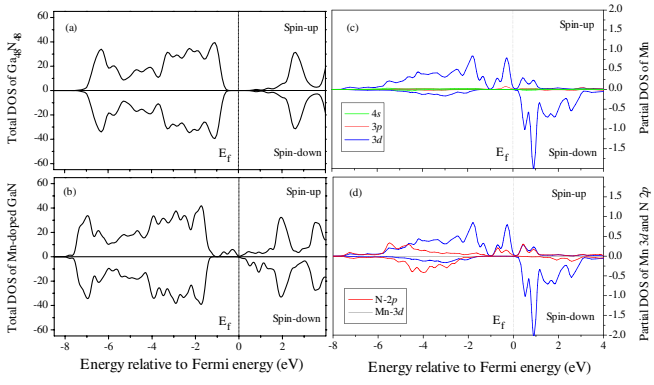

FIG. 3 (color online). (a) Total DOS corresponding to pure nanowire $Ga_{48}N_{48}$ supercell, (b) total DOS of Mn-doped GaN nanowire, (c) partial spin DOS of Mn in $Ga_{46}Mn_2N_{48}$, (d) partial spin DOS of Mn $3d$ and N $2p$ in $Ga_{46}Mn_2N_{48}$.

TABLE I. The energy difference ΔE_0 (ΔE) between AFM and FM states ($\Delta E = E_{\mathrm{AFM}} - E_{\mathrm{FM}}$ in eV) without (with) structure relaxation, the relative energy $\Delta\varepsilon$ (eV) calculated with respect to the ground state (configuration V), the optimized Mn-N and Mn-Mn distances (Å), and the magnetic moments (μ_{B}) at each Mn and its nearest neighbor N atoms for the configurations given in Fig. 2.

Configs.	ΔE_0	ΔE	$\Delta\varepsilon$	Coupling	$d_{\mathrm{Mn\text{-}N}}$	$d_{\mathrm{Mn\text{-}Mn}}$	μ_{Mn1}	μ_{Mn2}	μ_{N}
I	0.128	0.162	1.458	FM	1.913	3.075	3.388	3.443	−0.0121
II	−0.008	−0.363	0.617	AFM	1.774	2.755	2.165	−3.688	−0.050
III	0.051	−0.140	0.660	AFM	1.818	2.677	2.706	−2.930	−0.025
IV	0.104	0.067	0.191	FM	1.834	3.293	3.194	3.184	−0.090
V	0.197	0.075	0.000	FM	1.839	2.965	3.488	3.250	−0.114
VI	0.042	0.020	0.283	FM	1.837	5.190	3.269	3.269	−0.020

FM state. In this configuration the two Mn atoms reside in the outermost surface sites along [0001] direction. The Mn-N-Mn atoms form a zigzag chain with an angle $\angle$Mn-N-Mn = 108.66°. The Mn-Mn distance is 2.965 Å, and Mn-N bond length is 1.839 Å in the [0001] direction. The next two higher energy configurations (IV and VI) which lie 0.191 eV and 0.283 eV above the ground state are also FM. For these two configurations the Mn-N distances are nearly the same as that in the ground state configuration, namely, 1.84 Å, but the Mn-Mn distances are very different, namely, 3.293 Å and 5.190 Å. This could imply that the Mn-N distance may play a more crucial role than the Mn-Mn distance in dictating the magnetic coupling between the two Mn atoms. To explore this further, we note that Mn-Mn and Mn-N distances in bulk GaN (which is FM) are 3.23 Å and 1.99 Å while in Mn-doped $(11\bar{2}0)$ GaN thin film (which is AFM) they are 2.978 Å and 1.822 Å, respectively [36]. It is interesting that the Mn-N distances in configurations II and III (which are AFM) are also less than 1.82 Å (see Table I). All these results have one common feature: the configurations are FM when the Mn-N distance exceeds some critical value.

To gain further insight into the origin of FM coupling in Mn-doped GaN nanowire we plot in Fig. 3(b) the total DOS of $Ga_{46}Mn_2N_{48}$ supercell. Note that the Fermi energy passes through the gap in the spin-down DOS and the system behaves as half-metallic. The role of N in mediating the magnetic coupling between Mn atoms can be seen from Fig. 3(d) where the N $2p$ states overlap with the Mn $3d$ states. We see from Fig. 3(c) that much of the contribution to the magnetic moment comes from the Mn $3d$ electrons. The impurity states of doped Mn are in the gap region and are indicators of a double exchange mechanism [37,38]. This character is further confirmed from the DOS overlap in Fig. 3(d) and charge overlap between Mn-$3d$ and N-$2p$ orbitals. The Mn atoms are aligned ferromagnetically. Because of the different distances between the Mn atoms from the mediating N atom, the two Mn atoms are not equivalent and carry slightly different magnetic moment, namely $3.49\mu_{\mathrm{B}}$ and $3.25\mu_{\mathrm{B}}$. The magnetic moment at the N site linking the two Mn atoms is aligned antiferromagnetically to that of the Mn atoms. The moment at the N atom, however, is quite small, namely $-0.114\mu_{\mathrm{B}}$. This feature was also seen Mn_2N cluster where the two Mn atoms are coupled ferromagnetically while they are antiferromagnetically coupled to N [39]. The interaction of Mn with N is also confirmed from the charge density distribution in the Mn-N-Mn plane. We found that the charge buildup along the Mn-N-Mn bonds is much larger than that along the Ga-N-Ga bond. Consequently, the FM coupling between the two Mn atoms is mediated via the N atom. Since the two Mn atoms are not equivalent they carry different magnetic moments as well as charge. We thus ascribe the magnetism in Mn-doped GaN nanowire to be due to a double exchange mechanism, as is the case with Mn-doped GaN bulk [37,38,40,41].

Our results in Table I also help to shed light on the preferred distribution of Mn in GaN nanowire. Note that the energies of configurations IV and VI differ little from that of the ground state configuration V. All these configurations are FM with Mn-Mn distances ranging from 2.97 Å to 5.19 Å. We also note that among the six configurations studied, four exhibit FM while the other two exhibit AFM coupling. The Mn-Mn distances in the antiferromagnetically coupled configurations are always smaller than those in the FM configurations. The fact that the low energy configurations are FM where Mn atoms occupy different sites indicates that clustering is not associated with the FM coupling in the nanowire. To obtain the preferred direction of the magnetic alignment we have calculated the magnetic anisotropic energy with two Mn magnetic moments oriented along $[10\bar{1}0]$, [0001], and $[01\bar{1}0]$ directions. The magnetic alignment along the $[10\bar{1}0]$ direction in the wire is found to be 3.2 meV and 1.8 meV lower in energy than that along the [0001] and $[01\bar{1}0]$ directions, respectively. These energies are comparable to the values for Fe_2 molecule [42].

To study the effect of the wire diameter on the magnetic properties of Mn-doped GaN nanowire, we performed the calculations for the thinnest GaN nanowire which has been created from a wurtzite GaN ($5 \times 5 \times 4$) supercell by cutting the part outside of the innermost hexagonal unit along [0001] direction. The corresponding supercell consists of 48 atoms ($Ga_{24}N_{24}$) with a diameter of 0.45 nm and a length of 2.1 nm (as shown in Fig. 4). A vacuum space of 12.68 Å along both $[10\bar{1}0]$ and $[01\bar{1}0]$ directions in the

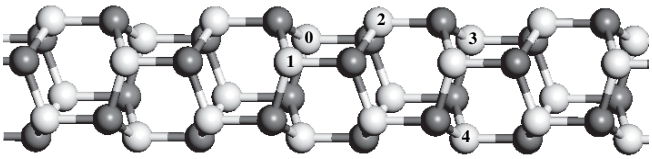

FIG. 4. Schematic representation of the $Ga_{24}N_{24}$ supercell. The lighter spheres are Ga and the darker spheres are N. The atoms occupying sites marked 0 and 1 are along $[10\bar{1}0]$ direction and these occupying positions 3 and 0 are along $[0001]$ direction.

supercell separates the wires from each other. The nanowire generated has infinite length along the $[0001]$ direction. It is interesting to note that the surface of this thinnest wire consists of three hexagons, very similar to the zigzag $(3, 0)$ carbon nanotube. To check the magnetic coupling between Mn atoms, we have also replaced two of the Ga atoms with Mn for four different configurations: $(0, 1)$, $(0, 2)$, $(0, 3)$, and $(0, 4)$ as shown in Fig. 4, labeled, respectively, as configurations I, II, III, and IV in Table II. The calculations have been carried out the same way as described for the larger wire. It is found that configuration I is the ground state with FM state being lower in energy by 0.08 eV than the AFM state, similar to what we found in the previous thicker wire. The other three configurations are 0.327, 0.416, and 0.390 eV higher in energy, respectively, than the ground state configuration I. In configurations III and IV, because of the large Mn-Mn distances, FM and AFM states are nearly degenerate in energy. Due to the smaller size of the wire, the larger bond length contraction results in smaller magnetic moments on Mn sites; e.g., in the ground state, the two Mn atoms only carry magnetic moment of $0.604\mu_B$ and $0.555\mu_B$. These Mn moments are smaller than any existing values in bulk or thin films. Therefore, in 1D system the wire thickness can be used to control the magnitude of the magnetic moment.

In summary, we show that the magnetic coupling between Mn atoms in GaN can be altered by suitably selecting the dimensionality of the system. In one-dimensional Mn-doped GaN nanowire, the special topology of the surface and the confinement of electrons in the radial direction drive the coupling to be ferromagnetic while in thin films the Mn atoms couple antiferromagnetically. In addition, the magnitude of the magnetic moments can be tuned by changing the wire thickness. The flexibility of both controlling the magnetic coupling and magnetic moment by choosing the dimensionality and the size of the wire may be useful in practical applications.

TABLE II. The energy difference, DE (eV) between AFM and FM states, the relative energy $\Delta\varepsilon$ (eV) calculated with respect to the ground state (configuration I), the optimized Mn-Mn distances (Å), and the magnetic moments (μ_B) at each Mn and its nearest neighbor N atoms for configurations given in Fig. 4.

Configs.	ΔE	$\Delta\varepsilon$	μ_{Mn1}	μ_{Mn2}	Coupling	$d_{Mn\text{-}Mn}$
I (0, 1)	0.080	0.000	0.604	0.555	FM	2.277
II (0, 2)	−0.015	0.327	2.067	−2.100	AFM	2.929
III (0, 3)	−0.010	0.416	2.347	−2.133	FM ~ AFM	5.145
IV (0, 4)	0.002	0.390	2.284	2.191	FM ~ AFM	5.870

The work was supported in part by a grant from the Office of Naval Research. The authors thank Professor Y. Kawazoe for the support of supercomputing facility. We thank Dr. A. K. Rajagopal and Dr. S. D. Mahanti for many useful discussions.

[1] M. L. Reed *et al.*, Mater. Lett. **51**, 500 (2001).
[2] M. L. Reed *et al.*, Appl. Phys. Lett. **79**, 3473 (2001).
[3] S. Sonoda *et al.*, J. Cryst. Growth **237**, 1358 (2002).
[4] T. Sasaki *et al.*, J. Appl. Phys. **91**, 7911 (2002).
[5] G. T. Thaler *et al.*, Appl. Phys. Lett. **80**, 3964 (2002).
[6] J. M. Lee *et al.*, Microelectron. Eng. **69**, 283 (2003).
[7] P. P. Chen *et al.*, J. Cryst. Growth **251**, 331 (2003).
[8] S. S. Seo *et al.*, Appl. Phys. Lett. **82**, 4749 (2003).
[9] Y. Shon *et al.*, J. Appl. Phys. **93**, 1546 (2003).
[10] T. Kondo *et al.*, J. Cryst. Growth **237**, 1353 (2002).
[11] M. E. Overberg *et al.*, Appl. Phys. Lett. **79**, 1312 (2001).
[12] K. Sardar *et al.*, Solid State Commun. **125**, 55 (2003).
[13] S. Dhar *et al.*, Appl. Phys. Lett. **82**, 2077 (2003).
[14] S. Dhar *et al.*, Phys. Rev. B **67**, 165205 (2003).
[15] K. H. Ploog *et al.*, J. Vac. Sci. Technol. B **21**, 1756 (2003).
[16] M. Zajac *et al.*, Appl. Phys. Lett. **79**, 2432 (2001).
[17] K. Ando, Appl. Phys. Lett. **82**, 100 (2003).
[18] T. Graf *et al.*, Phys. Status Solidi B **239**, 277 (2003).
[19] S. J. Pearton *et al.*, J. Phys. Condens. Matter **16**, R209 (2004).
[20] J. C. Johnson *et al.*, Nat. Mater. **1**, 106 (2002).
[21] S. Han *et al.*, Chem. Phys. Lett. **389**, 176 (2004).
[22] W. Han *et al.*, Science **277**, 1287 (1997).
[23] G. Cheng *et al.*, Appl. Phys. Lett. **75**, 2455 (1999).
[24] X. Duan *et al.*, J. Am. Chem. Soc. **122**, 188 (2000).
[25] C. Tang *et al.*, Appl. Phys. Lett. **77**, 1961 (2000).
[26] M. He *et al.*, Appl. Phys. Lett. **77**, 3731 (2000).
[27] W.-Q. Han *et al.*, Appl. Phys. Lett. **81**, 5051 (2002).
[28] J.-Y. Li *et al.*, Chem. Mater. **16**, 1633 (2004).
[29] F. L. Deepak *et al.*, Chem. Phys. Lett. **374**, 314 (2003).
[30] D. S. Han *et al.*, Appl. Phys. Lett. **86**, 032506 (2005).
[31] H.-J. Choi *et al.*, Adv. Mater. **17**, 1351 (2005).
[32] G. Kresse and J. Furthmüller, Phys. Rev. B **54**, 011169 (1996).
[33] Y. Wang and J. P. Perdew, Phys. Rev. B **44**, 013298 (1991).
[34] G. Kresse and J. Joubert, Phys. Rev. B **59**, 1758 (1999).
[35] Q. Wang *et al.*, Phys. Rev. B **72**, 045435 (2005).
[36] Q. Wang *et al.*, Phys. Rev. Lett. **93**, 155501 (2004).
[37] K. Satoa *et al.*, Physica B (Amsterdam) **340-342**, 863 (2003).
[38] K. Satoa *et al.*, Europhys Lett. **61**, 403 (2003).
[39] B. K Rao and P. Jena, Phys. Rev. Lett. **89**, 185504 (2002).
[40] P. M. Krstajic *et al.*, Phys. Rev. B **70**, 195215 (2004).
[41] H. Akai, Phys. Rev. Lett. **81**, 3002 (1998).
[42] J. Kortus *et al.*, Appl. Phys. Lett. **80**, 4193 (2002).